Development of Cell Surface Linkage Complexes in Cultured Fibroblasts

WEN-TIEN CHEN,*‡ ETSUKO HASEGAWA,‡§ TAKAYUKI HASEGAWA,§
CATHERINE WEINSTOCK,*‡ and KENNETH M. YAMADA§
*Department of Anatomy, Georgetown University Medical Center, Washington, DC 20007; ‡Howard
University Cancer Center, Washington, DC 20060; and §Laboratory of Molecular Biology, National Cancer
Institute, Bethesda, Maryland 20205

ABSTRACT   The possible role of a 140K membrane-associated protein complex (140K) in fibronectin-cytoskeleton associations has been examined. The 140K was identifed by the monoclonal antibody JG22E. Monoclonal and polyclonal antibodies to the 140K showed identical patterns of binding to the cell membranes of fixed and permeabilized chicken embryonic fibroblasts; localization was diffuse, but with marked concentration in cell-to-extracellular matrix contact sites. Correlative localization with interference reflection microscopy and double-label or triple-label immunofluorescence showed that 140K co-distributed with extracellular fibronectin fibrils and intracellular α-actinin in microfilament bundles at extracellular matrix contact sites but tended not to co-localize with tropomyosin present in bundles at sites farther from adhesion sites. In addition, binding of antibodies to 140K, α-actinin, and fibronectin was excluded from vinculin-rich focal adhesion sites at the cellular periphery. A progressive development of cell surface α-actinin–140K–fibronectin associations was observed in early spreading cells. The anti–140K monoclonal antibody JG22E inhibited the attachment and spreading of both normal and Rous sarcoma virus–transformed chicken embryonic fibroblasts to a fibronectin substratum. However, the anti–140K monoclonal antibody became a positive mediator of cell attachment and spreading if it was adsorbed or cross-linked to the substratum. Our results provide the first description of a membrane-associated protein complex that co-localizes with fibronectin and microfilament bundles, and they suggest that the 140K complex may be part of a cell surface linkage between fibronectin and the cytoskeleton.

Interactions of cells with extracellular materials are critically important events during embryonic development and for the maintenance of normal tissue functions. Fibronectin has been shown to promote the adhesion and spreading of cells on a variety of materials including plastic, collagen, gelatin, and fibrin (for reviews, see references 15, 22, 26, 31, 37, and 47). Concomitant with the spreading induced by added fibronectin, cells often acquire highly ordered intracellular microfilament bundles (MFBs)[1] (1, 45). In highly spread cells, extracellular matrix (ECM) fibers that contain fibronectin are often

observed to correspond in their arrangement with intracellular MFBs (20, 23, 39). At sites where ECM fibrils appear to attach to the plasma membrane, there is a co-distribution of actin and α-actinin (and sometimes vinculin) inside cells and fibronectin outside cells (4, 9, 24, 40, 41).

Immunoelectron microscopy has shown a spatial relationship between fibronectin and α-actinin at membrane attachment sites in spread fibroblasts, which were termed ECM contacts (10). These results suggest that there may be some form of physical connection at the ECM contacts between the ECM and the MFB (22, 40, 42). A number of investigators have postulated the existence of transmembrane molecules that connect these two assemblies, none of which have yet been identified. The idea that a transmembrane linkage complex exists at the ECM contacts has important implications

---

[1] Abbreviations used in this paper: CEF, chicken embryo fibroblasts; CEL, chicken embryonic lung; ECM, extracellular matrix; IRM, interference reflection microscopy; 140K, a three component, membrane-associated protein complex; MFB, microfilament bundle; RSV, Rous sarcoma virus.

for considerations of the effects on ECMs on cellular behavior (26, 42, 43).

To identify integral membrane molecules involved in such a transmembrane linkage, we have taken an immunological approach that comprises cytochemical localization, biochemical analysis of the antigen, and functional assays. In principle, monoclonal antibodies can be produced against impure cell membrane preparations and selected on the basis of their specific localization to particular cell contact sites in immunocytochemical experiments (42) or their biological effects in disrupting cell-ECM adhesions (17, 21, 32, 33, 44). The antigens to which such antibodies are directed can be then identified and characterized.

Greve and Gottlieb (17) reported that a particular monoclonal antibody, JG22, which was prepared against chick myogenic cells, had the unusual property of causing myoblasts, but not fibroblasts, to detach from substrata. Immunoelectron microscopic labeling experiments were later performed on several types of cells and tissues with the JG22 monoclonal antibody (8, 12), that showed specific localization to the plasma membrane, particularly in close contacts and ECM contacts of fibroblast-substratum interfaces and in the basolateral membranes of intestinal epithelial cells. A tentative identification of the antigen recognized by JG22 with monoclonal antibody affinity chromatography and SDS-gel electrophoresis (6, 8, 17) showed a diffusely stained band of ~140,000 mol wt (termed 140K), but further characterization of the antigen was hampered because the hybridoma that produces JG22 became unstable. We obtained new clones and further characterized this interesting antigen, with emphasis on new biochemical, immunocytochemical, and functional analyses. Our results suggest that this antigen is involved in the transmembrane association of extracellular fibronectin and the cytoskeleton.

MATERIALS AND METHODS

Cell Culture and Indirect Double Immunofluorescence: Chicken embryonic fibroblasts (CEF), chicken embryonic lung (CEL) cells, and cells transformed by the Schmidt-Ruppin strain of Rous sarcoma virus (RSV) were obtained and cultured in Dulbecco's modified Eagle's medium that contained 4.5 g/liter glucose, 10% fetal calf serum, 10 μg/ml gentamycin, and 2 mM glutamine, as described (10, 11). Cells on glass coverslips were usually cultured for 6 h, fixed with 3% paraformaldehyde, permeabilized with 0.4% Triton X-100, and double-immunolabeled according to the two-stage labeling procedure previously described (10). Each antibody was applied at a concentration of 10 μg/ml. Briefly, the first stage of the procedure applied to the cells was either a mixture of mouse JG22E monoclonal antibody and rabbit anti-fibronectin antibody, or a mixture of rabbit anti-140K antibody and guinea pig anti-fibronectin antibody. With intervening washing, the second stage of the procedure consisted of either a mixture of affinity-purified rhodamine conjugates of goat antibody against mouse IgG, and fluorescein conjugates of goat antibody against rabbit IgG; or a mixture of rhodamine conjugates of goat antibody against guinea pig IgG, and fluorescein conjugates of goat antibody against rabbit IgG. The secondary goat antibodies were prepared and affinity purified on the appropriate immunoadsorbant, then cross-absorbed against the heterologous antigens in each labeling procedure.

Several types of control experiments were performed in double-immunolabeling procedures. (a) An excess of purified antigen (fibronectin or 140K) at 100 μg/ml was added together with the primary antibody mixtures to compete specifically for the labeling of that antigen (e.g., Fig. 2h). (b) The appropriate preimmune or nonimmune rabbit, guinea pig, or mouse IgG was substituted for each primary antibody. (c) For the labeling with rabbit anti-140K polyclonal antibody, the antibody was cross-absorbed against fibronectin-Sepharose before the double-labeling procedure to avoid any possibility of contamination by antibody to fibronectin (Fig. 2k), though none was detected by immunoblotting. In each of these cases, the controls showed negligible labeling. In addition, experiments were done in which the primary antibodies to a pair of antigens remained the same but the secondary antibody conjugates were reversed, to

show that the labeling pattern of the two antigens was specific.

Correlative Localization by Interference Reflection Microscopy (IRM) and Triple-label Immunofluorescence: CEL cells cultured on 22-mm glass coverslips for 1 d were fixed, permeabilized, and double-immunolabeled with a mixture of primary antibodies (JG22E and rabbit anti–α-actinin or rabbit anti-tropomyosin), then with a mixture of secondary antibodies (rhodamine conjugates of goat antibody against mouse IgG and fluorescein conjugates of goat antibody against rabbit IgG) as described above. The coverslip was incorporated into a filming chamber filled with phosphate-buffered saline (PBS), constructed from spacers of No. 2 coverslips attached to a glass slide and the coverslip by double-sided tape.

Labeled cells were photographed with an Antiflex 63/1.4 objective (Carl Zeiss, Inc., Thornwood, NY) on a Zeiss Photomicroscope III by IRM, then by epifluorescence microscopy for rhodamine labeling of 140K and fluorescein labeling of α-actinin or tropomyosin. Three fields of labeled cells were photographed for each coverslip, and their positions on the microscopic stage were recorded. The cells were then exposed to fluorescein-excitation illumination for an additional 3 min to photobleach all of this bound fluorochrome. The coverslips were then labeled with the third antibody (fluorescein conjugates of anti–fibronectin antibody, characterized in reference 46) in the filming chamber, and the cells were relocated on the microscopic stage for photography of the fibronectin labeling. Specificity controls for the three labeling steps in this procedure were the same as for the double-label experiment described above, and were all negative. Cross-reactivity among antibody reagents used in this triple-label experiment was negligible, and there was no fluorescence visible when cells were examined after the photobleaching step and before addition of the third label.

Antibody Production: The JG22 monoclonal antibody was originally obtained from a hybridoma derived from fusion of mouse plasmacytoma SP2/0 cells and spleen cells of a BALB/c mouse that had been immunized with 14-d chicken embryonic muscle tissue (17). To examine further the nature of the JG22 antigen, we re-cloned the original hybridoma that produced JG22, twice by limiting dilution and selected for new lines that secrete monoclonal antibody by use of immunofluorescent assays. The most extensively characterized new hybridoma clone, designated JG22E, is stable and appears to produce a monoclonal antibody with reactivity to the plasma membrane identical to that of JG22, based on its affinity to membrane extracts and immunocytochemical localization. The hybridoma JG22E line was cultured in serum-free HB101 medium (Hana Biologics, Berkeley, CA) and 1% penicillin-streptomycin mixture (Gibco Laboratories, Grand Island, NY). Antibody was purified by ammonium sulfate precipitation and DEAE chromatography. Approximately 80 mg of JG22E monoclonal antibodies was obtained from each liter of culture medium.

For production of polyclonal antibody to 140K in rabbits, the rabbit was immunized with JG22E-affinity-purified 140K. Aliquots of purified 140K in Ca^{++}- and Mg^{++}-free PBS that contained 100 μg protein were stored in liquid N_2 and thawed immediately before injection. The first three injections were subcutaneous on the back and footpads, 4 wk apart. The first injection was in complete Freund's adjuvant, the second in incomplete Freund's adjuvant, and the third in PBS. The animal was tested for antibody titer after the third injection. The antibody-producing animal was then bled from ear veins (~50 ml/mo) for purification and characterization of the antibody. Polyclonal rabbit antibody IgG was purified from the antisera on a Sepharose 4B-protein A (Pharmacia Fine Chemicals, Piscataway, NJ) column. A fraction of rabbit anti-140K antibody was further affinity purified on the 140K-Sepharose 4B column and cross-absorbed against a chicken cellular fibronectin column. This affinity-purified antibody to the 140K proteins showed the same immunofluorescent pattern as did protein A-purified antibody.

Membrane Extracts and JG22E Immunoaffinity Chromatography: To prepare JG22E antigen extracts, we homogenized 36 13-d chicken embryos in 400 ml cold 0.25 M sucrose in 10 mM Tris buffer, pH 7.4, plus 3 mM $CaCl_2$, 1 mM phenylmethylsulfonyl fluoride, and 1 mM benzethonium chloride, first in a Waring blender for 2 min, then by 13 strokes of a tight pestle of a Dounce homogenizer at 4°C after it was filtered through cheese cloth. The homogenate was centrifuged as described (17), and the resultant pellet (crude membrane fraction) was then extracted for 40 min with 50 ml of 40 mM octyl-β-D-glucopyranoside in 50 mM Tris buffer, pH 7.4, plus 3 mM $CaCl_2$, and 1 mM phenylmethylsulfonyl fluoride. The detergent extract was centrifuged for 60 min at 100,000 g, and the pellet was discarded. JG22E monoclonal antibody was coupled to CNBr-activated Sepharose 4B for affinity purification of JG22E antigen from the octyl-β-D-glucopyranoside extracts. For each experiment, 50 ml of octyl-β-D-glucopyranoside extract supernatant solution was incubated with 5 ml of either control mouse IgG or JG22E-Sepharose (70 mg total IgG coupled) overnight at 4°C in slowly rotating tubes. The beads were washed with 300 ml of the extraction solution and then packed into columns. The columns were eluted with 2.4 column vol of 50 mM diethyl-

amine, pH 11.5, plus 40 mM octyl-β-D-glucopyranoside, 1 mM $CaCl_2$, and 1 mM phenylmethylsulfonyl fluoride. The purified 140K preparation was used either for polyclonal antibody production in rabbits or SDS-gel analysis. Samples were analyzed on 7.5% SDS-polyacrylamide gels with (Fig. 1, lane a) or without (Fig. 1, lane b) reduction by 0.1 M dithiothreitol. For Western immunoblot analyses, gel bands were transferred to nitrocellulose in 5 mM sodium borate, pH 9.2, in a Trans-Blot apparatus (Bio-Rad Laboratories, Richmond, CA) for 2 h at 4°C. After incubation with 5% bovine serum albumin (BSA) overnight, blots were stained with rabbit antibody and then with [^{125}I]protein A (New England Nuclear, Boston, MA) as described (3).

Coating of Fibronectin or JG22E Monoclonal Antibody on Plastic Surfaces: Bovine plasma fibronectin was prepared by gelatin-affinity chromatography (38). Each well of Linbro 96-well tissue culture plates (Flow Laboratories, Inc., McLean, VA) was incubated with 100 μl of protein solution (fibronectin or JG22E) at concentrations of 0.02–2,000 μg/ml in PBS for 90 min, and then incubated with preheated BSA (3 min at 80°C) in PBS (3 mg/ml) for 60 min. Thereafter, the substratum surfaces were rinsed extensively with PBS for cellular adhesion assays.

Covalent Linkage of JG22E Monoclonal Antibody to Fixed Gelatin Surfaces: Purified JG22E was covalently linked to the surface of a fixed gelatin film according to a previously described procedure (10–12). Briefly, the gelatin solution (heat-denatured bovine type I collagen) was first coated on 96-well plates, and the film was fixed with 4% glutaraldehyde overnight. The free aldehyde groups on the surface of fixed gelatin film were coupled to JG22E at various concentrations, and then nonspecific binding sites were quenched and masked with 3% BSA plus 0.1 M glycine.

Assays for Cellular Adhesion and Spreading on Substrata: Cellular adhesion assays were performed on substrata either coated or coupled with various proteins in Linbro 96-well microtiter tissue culture plates (Flow Laboratories, Inc.). Subconfluent cell cultures were trypsinized, and the protease reaction was stopped with excess normal medium that contained 10% fetal calf serum. The cell suspension was placed into conical polypropylene tubes and was incubated at 37°C for 30 min to allow the cells to recover from proteolytic damage. For each adhesion assay, each well of pretreated 96-well plates was first filled with 50 μl of either normal medium or normal medium plus antibodies. An additional 50 μl of cell suspension that contained ~1 × 10^3 cells was added to each well. The plate was then incubated at 10% CO_2 and 37°C for 30 min, and the attached cells were fixed with 100 μl of 4% glutaraldehyde in PBS for 30 min. The wells in the plate were rinsed with distilled water, dehydrated with ethanol, and then air dried. The attached cells on each well were counted and photographed with a Nikon Diaphot inverted phase-contrast microscope (Nikon, Inc., Garden City, NY).

RESULTS

140K Membrane-associated Protein Complex

Monoclonal antibody JG22E was obtained from a new, stable subclone of the JG22 hybridoma (see Materials and Methods). The identity of the antigen recognized by the JG22E monoclonal antibody was investigated by affinity chromatography of Nonidet P40 or octylglucoside detergent extracts of 13-d-old chicken embryo membranes (see Materials and Methods). Purified antigen was used for either polyclonal antibody production in rabbits or SDS-gel analysis. When the antigen was analyzed by electrophoresis on a 7.5% SDS-polyacrylamide gel without reduction (Fig. 1, lane b), the sample could be resolved into three major, distinct bands stained by Coomassie Blue, with apparent molecular weights of 155,000, 135,000, and 120,000, plus a variable minor band of 167,000, rather than a single broad 140,000-mol-wt band as originally observed (17). However, if the antigen was exposed to 0.1 M dithiothreitol before SDS PAGE, two bands in the molecular weight range of 150,000 and 125,000, plus the minor band at 175,000 (Fig. 1, lane a), were observed. Except for the variable, minor band at 170,000 mol wt, this set of bands isolated from chicken embryo membranes appears to be similar to the antigen of cultured CEF recognized by another monoclonal antibody, termed CSAT produced in another laboratory (29, 30, 32).
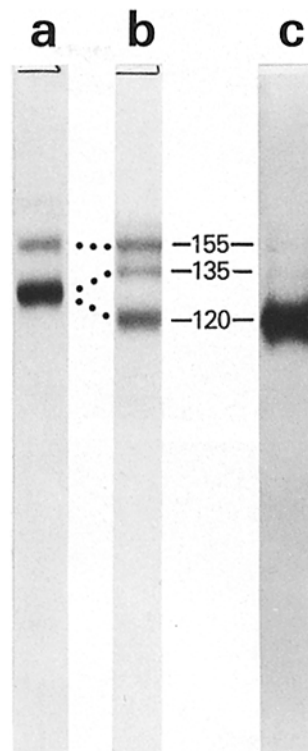

FIGURE 1 Lanes a and b, polypeptides from JG22E-affinity-purified antigen that were analyzed by electrophoresis on a 7.5% SDS-polyacrylamide gel with (lane a) or without (lane b) reduction by 0.1 M dithiothreitol. Dotted lines indicate migration of each component as deduced by reduction and re-electrophoresis of each band that was excised from the nonreducing gel in a separate experiment. Lane c, Western immunoblot of the rabbit polyclonal anti-140K antibody against the 140K complex applied at a 1:50 dilution of anti-140K antibody. Apparent molecular weights were determined by matching the autoradiogram with 140K and molecular weight standards stained with amido black in other lanes of the same gel transfer. Note that most reactivity is against the lowest 120,000-mol-wt component (120), although some antibodies bind to the other two bands in low amounts. 155, 155,000 mol wt; 135, 135,000 mol wt; 120, 120,000 mol wt. Molecular weight standards included myosin (200,000), RNA polymerase (160,000 and 150,000), β-galactosidase (116,000), phosphorylase b (94,000), BSA (68,000), ovalbumin (43,000), and carbonic anhydrase (30,000).

The three components visualized by nonreduced SDS-gel electrophoresis, i.e., 155,000, 135,000, and 120,000 mol wt (collectively designated 140K), appear to exist as a membrane-associated protein complex under physiological conditions. They are always co-purified by affinity chromatography, and we have thus far been unable to separate the three components under various nondenaturing conditions by sucrose density gradients, molecular sieving, anion exchange, and lectin-affinity chromatography. In addition, treatment of crude membrane preparations with 1 M urea, 3 M KCl, or hypotonic shock before detergent solubilization and purification of the antigen does not alter the SDS gel profiles (data not shown). Similar evidence for a glycoprotein complex with similar components has also been reported by Knudsen et al. (29). These data suggest a membrane association for one or more components of the 140K and are consistent with the results of a previous immunoelectron microscopic study using an ultrathin frozen-sectioning method that showed specific location of the 140K on the plasma membrane (12). In an analysis of the chemical nature of 140K to be published elsewhere (Hasegawa, T., E. Hasegawa, W.-T. Chen, and K. M. Yamada, manuscript submitted for publication), it was found that the two-dimensional peptide maps of all three bands were distinct. This result suggests that the three bands of 140K are not proteolytic fragments of one another.

Immunocytochemical experiments using a combination of monoclonal and polyclonal antibodies were done to explore the possible relationship between the 140K complex and fibronectin. To decrease the possibility of immunological artifacts, we tested both types of antibodies. The polyclonal
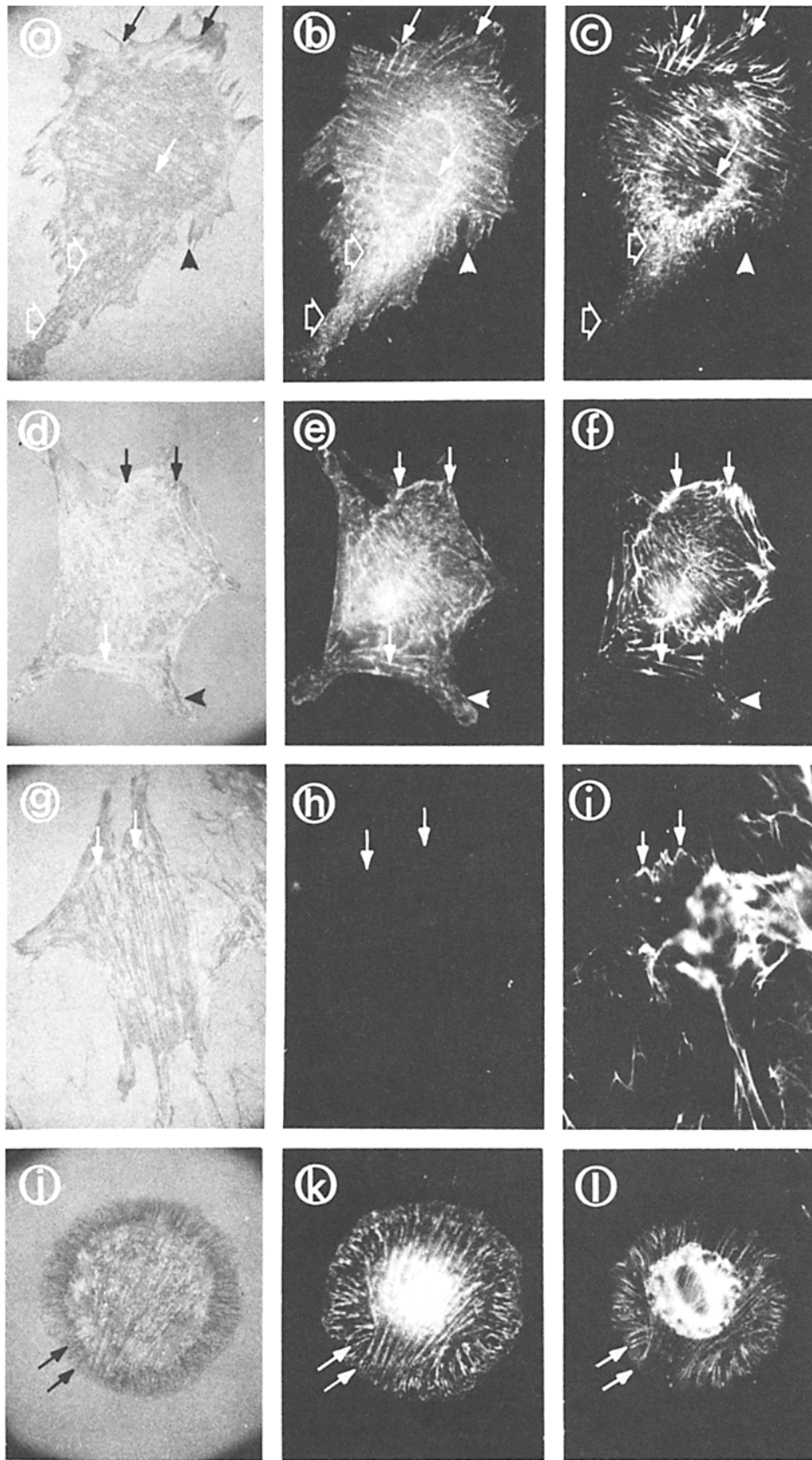
FIGURE 2 Detection of 140K membrane complexes and co-localization of 140K with fibronectin fibrils. a, d, g, and j show IRM images of four CEFs contacting a glass substratum after 6 h in culture; b, e, h, and k are the same cells viewed with immunofluorescent labeling for 140K; c, f, i, and l are the same cells labeled for fibronectin. (a, b, and c) IRM (a) and indirect double-immunofluorescent labeling with JG22E monoclonal antibody for 140K (b) and with anti–fibronectin antibody for fibronectin (c) of the same cell. Arrows point to ECM contacts formed between the plasma membrane and fibronectin fibrils (a) that label for both 140K (b) and fibronectin (c). Arrowheads indicate the focal adhesion sites (a) where both 140K (b) and fibronectin (c) are absent, but both 140K and fibronectin are present immediately surrounding these focal adhesions. Open arrows point to the broad area of close contacts (a) that show low levels of diffuse 140K (b) and fibronectin (c). (d–f) IRM (d) and indirect double-immunofluorescent labeling with rabbit polyclonal antibody against JG22E-affinity-purified 140K (e) and guinea pig polyclonal antibody against fibronectin (f). Solid arrows point to ECM contacts and solid arrowheads point to focal adhesion sites (d) that show co-localizations of 140K (e) and fibronectin (f) similar to those in a–c. (g–i) IRM (g) and indirect double-immunofluorescent labeling in a control in which rabbit anti–140K antibodies were previously reacted with purified 140K preparation (h), as compared with fibronectin labeling of the same cell (i). Arrows indicate the ECM contacts (g) that are negative for 140K labeling due to competition by purified 140K (h), but positive for fibronectin (i). (j–l) IRM (j) and indirect double-immunofluorescent labeling for a control in which rabbit anti–140K antibodies were previously absorbed with excess fibronectin (k), and fibronectin labeling of the same cell (l). × 520.

rabbit antibody against JG22E–affinity-purified 140K reacted primarily against the smallest (120,000 mol wt) component in Western immunoblots, but small amounts of reactivity against the other three bands were also detected (Fig. 1c). Both the polyclonal antibody against 140K and the monoclo-

nal JG22E antibody displayed a distinctive immunofluorescent-labeling pattern in CEF cells that consisted of a combination of diffuse labeling of the cell membrane and localized streaks at ECM contacts (Fig. 2, b and e). In other experiments, a mixture of fluorescein conjugates of JG22E and
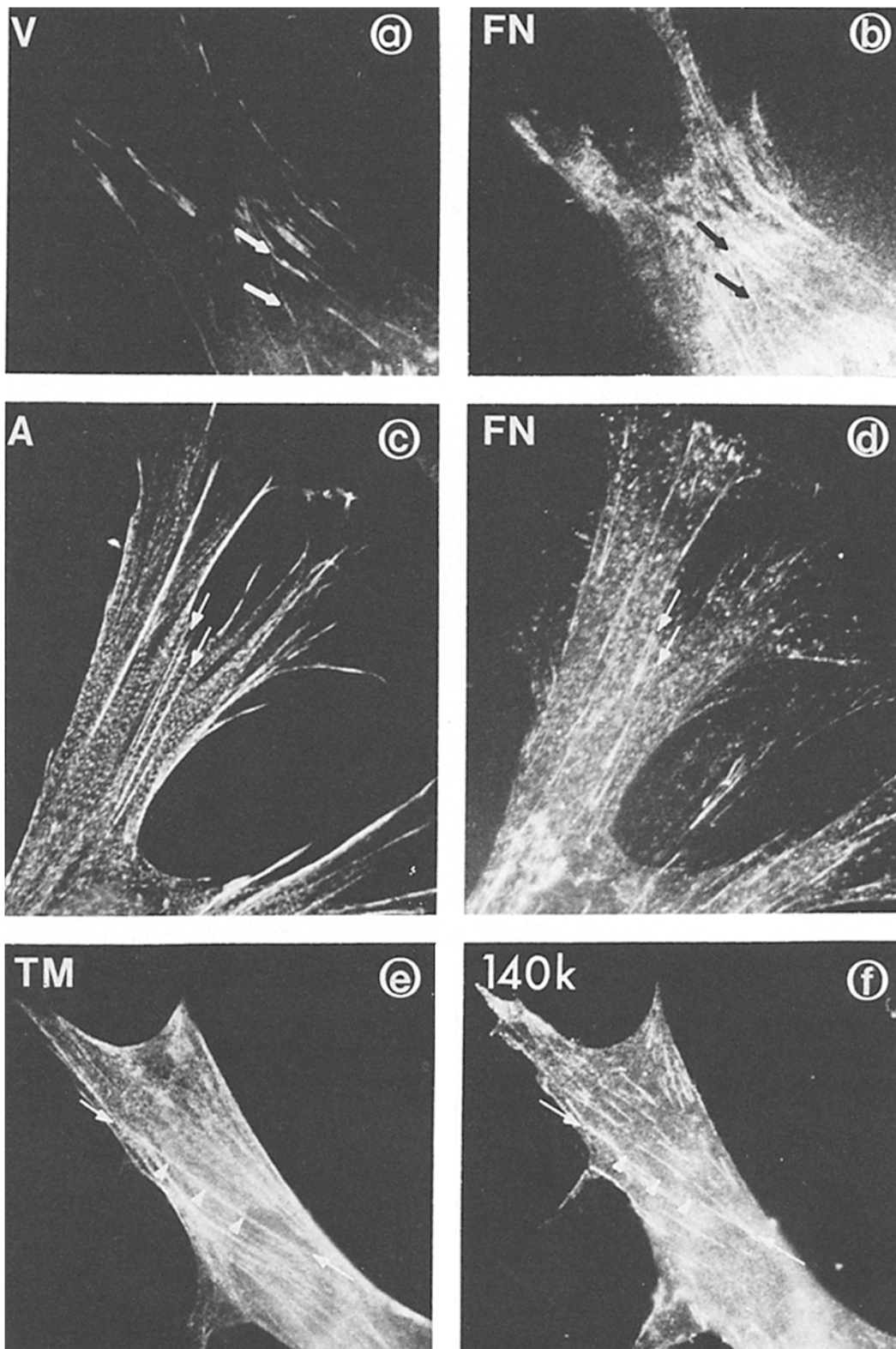
FIGURE 3   Co-distribution of fibronectin fibrils, 140K, and MFBs at ECM contacts. (a and b) Double-immunofluorescent labeling for vinculin (V) and fibronectin (FN) of a CEL cell. Arrows mark some of the coincidences. (c and d) Double-immunofluorescent labeling for α-actinin (A) and fibronectin (FN) of a CEL cell. Arrows indicate two areas where MFBs are co-linear with fibronectin fibrils. (e and f) Double labeling for tropomyosin (TM) and 140K proteins (140K) of a CEL cell. Arrows point to a linear region of microfilament-membrane attachment that is labeled for 140K proteins with JG22E monoclonal antibody; TM labeling is present in this region, although it is not clear whether labeling for 140K and TM coincide precisely. Arrows indicate regions in MFBs farther from their membrane attachment sites, which remain labeled for TM (16) but show no labeling for 140K. × 1,200.

rhodamine conjugates of anti–140K polyclonal antibody was applied to the same cells, and it showed identical localization patterns.

Possible antigenic relationships between the 140K and fibronectin were ruled out by double-immunofluorescent labeling of the whole CEF preparations. Polyclonal rabbit antibodies against 140K were first absorbed with chicken cellular fibronectin immobilized on Sepharose beads. A mixture of these fibronectin-absorbed polyclonal rabbit antibodies against 140K and polyclonal guinea pig antibodies monospecific for fibronectin was added to the cells, and then the appropriate two secondary-labeling reagents were applied as described in Materials and Methods. If antibodies to 140K were directed to antigenic determinants on the fibronectin molecule, or if antibodies to fibronectin were directed to 140K, the double labeling that results might be identical. However, total identity was not observed (Fig. 2, k and l). The two immunofluorescent-labeling patterns on the cell surfaces were quite distinct, with that for 140K (Fig. 2 k) being much more disperse and punctate on the cell membrane than was the labeling pattern for fibronectin. Moreover, extracellular fibrils of fibronectin located away from the cell body (e.g., to the right of the right upper arrow in Fig. 2, e and f) did not stain with 140K antibodies. In addition, the intensity of anti–140K labeling was significantly affected by neither the prior absorption of 140K antibodies with fibronectin nor mixing with potentially competing antibodies to fibronectin during staining. Similar results were obtained in a comparison between the JG22E monoclonal antibodies and polyclonal rabbit antibodies monospecific for chicken cellular fibronectin. These experiments show that the antigen recognized by either anti–140K antibodies or JG22E is not immunochemically related to fibronectin and support the conclusion that 140K proteins are not proteolytic fragments of fibronectin.

## Localization of 140K in Cell Surface Linkage Complexes

By use of IRM and double-immunolabeling techniques, we focused on the localization of 140K and its possible co-localization with fibronectin or other cytoskeletal proteins at cell-ECM contact sites, briefly termed ECM contacts, the overall structure of which has been previously described at the ultrastructural level (10). In IRM, when such fibronectin-containing ECM contacts are close to the glass substratum (e.g., arrows in Fig. 2, a, g, and j, and in Figs. 4 and 5; arrow and arrowhead pairs in Figs. 6 d and 7 d), they appear as fine, elongated, dark streaks, and may be referred to as focal contacts in the central regions of cells (24, 40). In contrast, the focal contacts located at the periphery of the cell, often

referred to as focal adhesions (10, 22, 24, 27, 33, 40–42), appear as darker and wider IRM streaks (see Fig. 4, open arrows for focal adhesions and solid arrows for ECM contacts), and are not labeled for fibronectin (10, 24, 40). Careful examination of ECM sites that contain fibronectin that are co-aligned with intracellular microfilament bundles revealed regions of negative contrast streaks (arrows in Fig. 2 d; arrowheads in Figs. 4 and 5) that are ECM sites of wide separation (>50 nm) from the glass surface (see also references 10 and 27). It was often possible to trace fibronectin fibrils from such negative-contrast ECM sites to regions of very close apposition to the glass substratum, indicated by the IRM-dark streaks. The spanning of considerable distances by fibronectin fibrils attached to the substratum and to the cell surface close to microfilament bundles can be seen in a number of previous studies of fibronectin localization (e.g., see references 1, 4, 9, 10, 12, 15, 39, and 46).

Fig. 2 shows CEFs visualized by IRM (Fig. 2, a, d, g, and j) as compared with double-label immunofluorescence for 140K (Fig. 2, b, e, h, and k) and for fibronectin (Fig. 2, c, f, i, and l) within the same cells. Close examination of the results showed that the three patterns (IRM, 140K, and fibronectin) were all related at specific contact sites. Many apparent elongated 140K-fibronectin associations were found to be strikingly coincident with ECM contacts in the perinuclear region of CEF (elongated streaks marked by arrows in Fig. 2, a, d, g, and j). Other possible 140K-fibronectin associations were found in diffuse close contacts (open arrows in Fig. 2, a–c) and in areas immediately surrounding the focal contacts at cell margins (arrowheads in Fig. 2, a–f), as shown in a previous study (8, 12). However, neither 140K nor fibronectin was present within the focal contacts at the cell periphery, which were previously shown to be vinculin positive and fibronectin negative (2, 10, 40), nor were they detected on the dorsal (upper) surfaces of these cells.

In addition, possible spatial associations among some cytoskeletal proteins, 140K, and fibronectin at ECM contacts in CEL cells were examined by pairwise double-labeling for vinculin and fibronectin (Fig. 3, a and b), α-actinin and fibronectin (Fig. 3, c and d), vinculin and 140K, α-actinin and 140K, and tropomyosin and 140K (Fig. 3, e and f). Similar to observations in CEF, an apparent α-actinin–140K-fibronectin association was found in ECM contacts of CEL cells, as evidenced by striking co-localization. Vinculin and tropomyosin were located near α-actinin distribution along the ECM contacts, but not in identical patterns (not shown, see also reference 16). Clearly, extracellular fibronectin fibrils, the 140K antigen, and intracellular cytoskeletal fibers show a high degree of co-linearity, and the 140K may be in a position to connect the two linear arrays.

Figure 4   Coincident distribution of 140K, α-actinin (A), and fibronectin (FN) at ECM contact sites as revealed by IRM and triple-label immunofluorescence of CEL cells cultured for 1 d on glass coverslips. (Left panels) A polarized cell. Arrows point to ECM sites that contact the glass surface and are seen as fine, dark streaks by IRM, and that are labeled positively for 140K, A, and FN. Arrowheads point to ECM sites of wide separation from the substratum that are elongated streaks of negative contrast in IRM, and that are also labeled positively for 140K, A, and FN. Open arrows indicate the focal adhesion sites in IRM where A appears to be present; in contrast, by the limited resolution of light microscopy, both 140K and FN appear to surround, but not enter, these focal contacts. (Right panels) A nonpolarized, well-spread cell. Open arrows indicate a focal adhesion in IRM that is labeled negatively for 140K, A, and FN. Arrowheads point to ECM sites immediately adjacent to the focal adhesion that are negative-IRM contrast streaks, and that are labeled positively for 140K, A, and FN. Examples of ECM sites in contact with the substratum are shown by arrows. × 1,200.
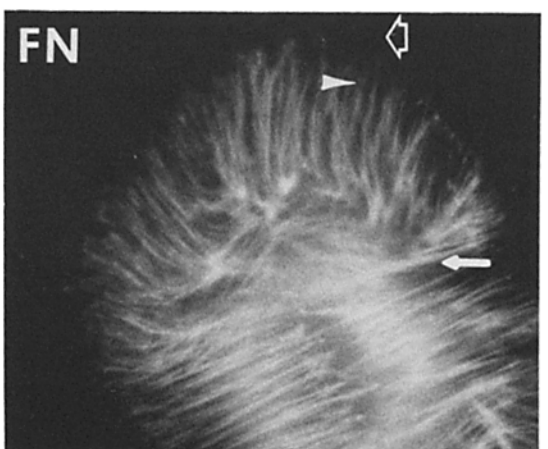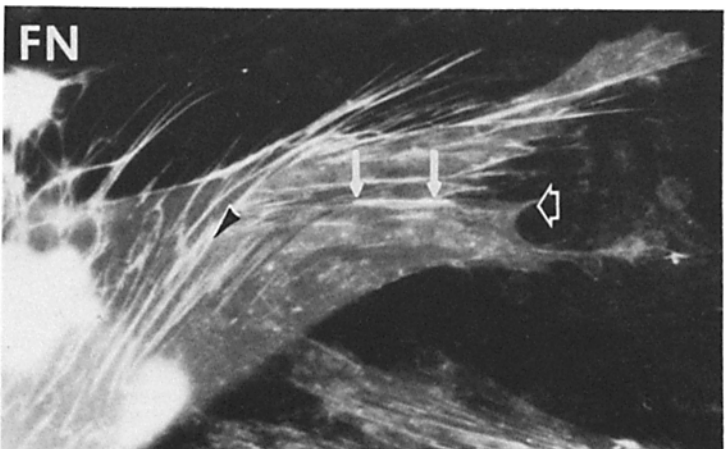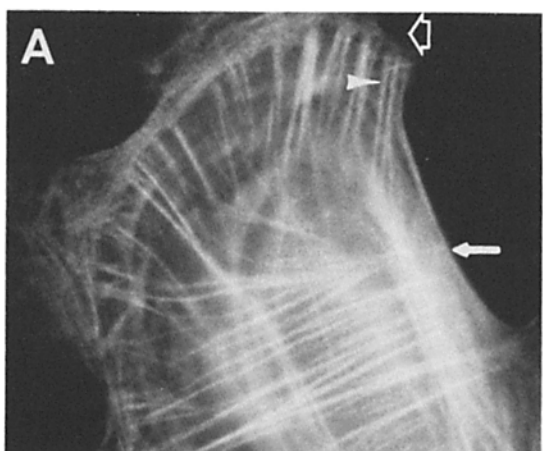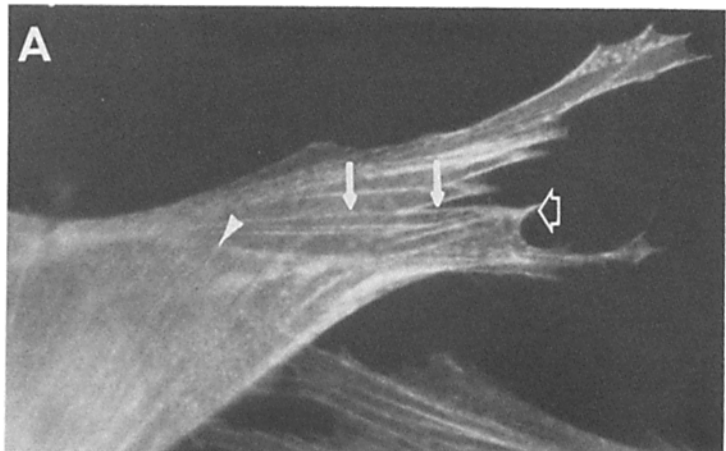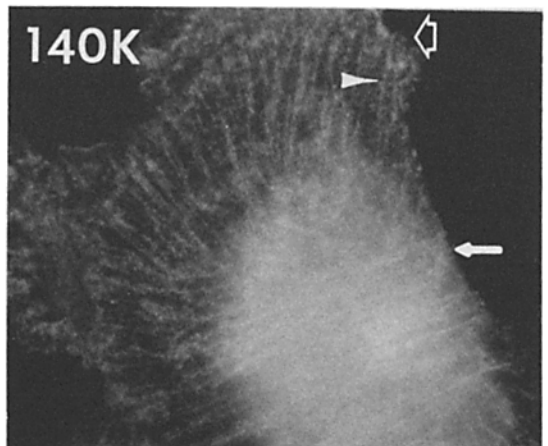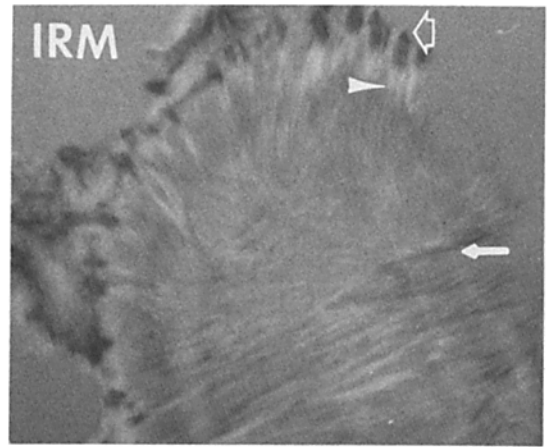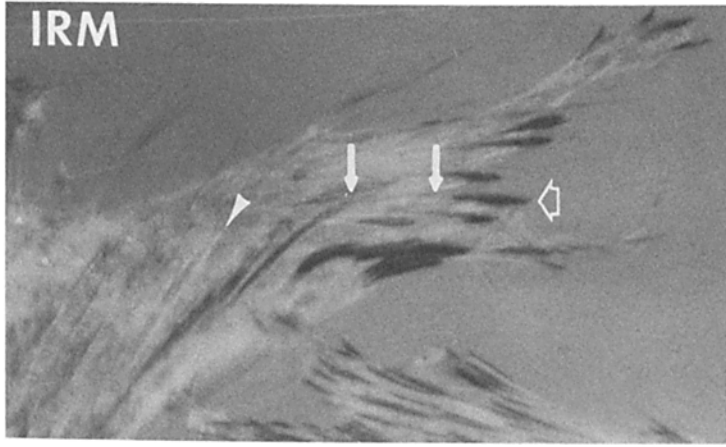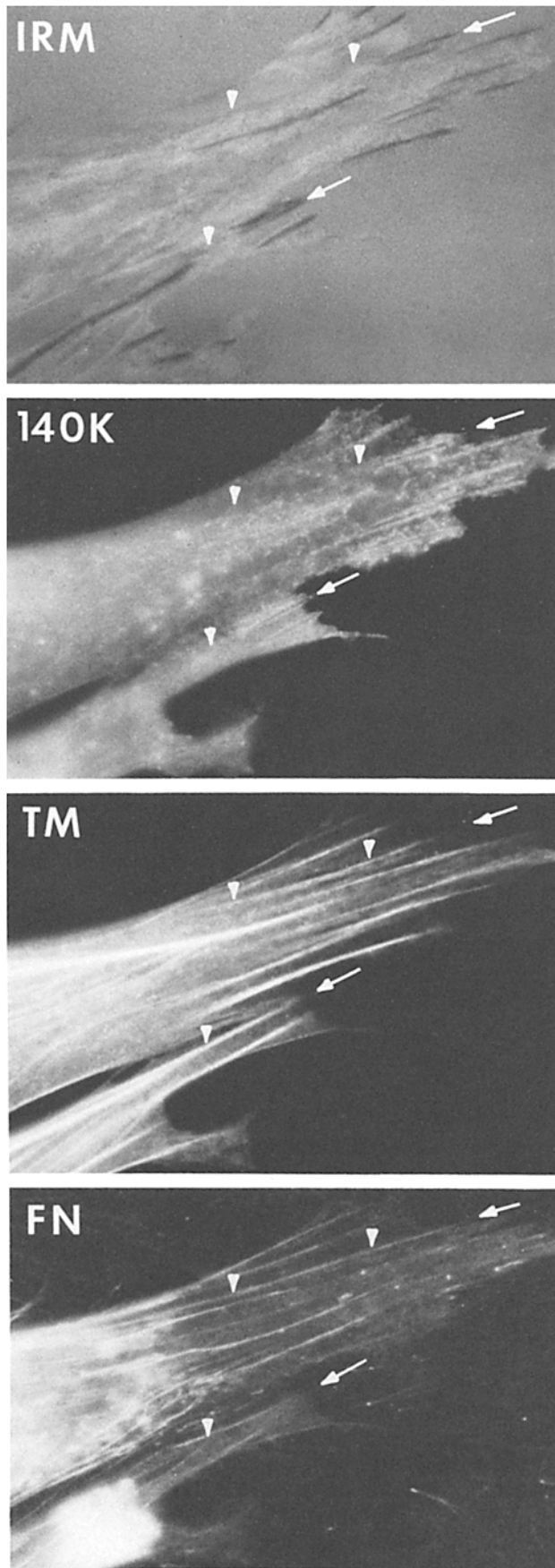
Demonstration of 140K, α-Actinin, and Fibronectin Co-localization at ECM Contacts

The double-label experiments described above showed a close spatial association of 140K with fibronectin and of fibronectin with α-actinin at ECM contacts. However, the 140K-fibronectin–labeled fibers might not have been the same fibers that stained for fibronectin and α-actinin. To determine whether 140K, α-actinin, and fibronectin co-align in identical ECM contacts in the same cells, we performed triple-label immunofluorescence experiments for 140K, fibronectin, and α-actinin or tropomyosin, and related their co-localization with the ECM contacts of the same cells as revealed by IRM, by use of the procedure outlined in Materials and Methods.

Fig. 4 shows CEL cells visualized by IRM as compared with triple-labeling for 140K, fibronectin, and α-actinin within the same cells, whereas Fig. 5 shows a similar preparation of CEL cells, but triple-labeled for 140K, fibronectin, and tropomyosin. Close examination of the results showed that three of these proteins (140K, α-actinin, and fibronectin) were all related at specific contact sites revealed by IRM, as found in previous double-label experiments. Many apparent 140K–α-actinin–fibronectin associations were found to be coincident with dark elongated IRM streaks which indicated attachment of ECM contacts to the glass surface (arrows in Fig. 4), and with negative-contrast IRM streaks showed wide separation of ECM contacts from the substratum (arrowheads in Fig. 4). Other 140K–α-actinin–fibronectin associations were found in areas immediately surrounding the focal contacts at cell margins (open arrows in the left panel of Fig. 4) but were not present within the focal contacts themselves (all open arrows in Fig. 4). Co-localization of tropomyosin, 140K, and fibronectin was found reproducibly only in limited portions of microfilament bundles as they approached the focal contact regions detected by IRM. In contrast, other regions of microfilament bundles that were distant from the substratum attachment sites visualized by IRM showed no association with 140K, even though they remained positively labeled for tropomyosin, or sometimes with fibronectin (arrowheads in Figs. 3 and 5). These results strongly suggested that 140K co-distributed with extracellular fibronectin fibrils and intracellular α-actinin in microfilament bundles at ECM sites, but tended not to co-localize with tropomyosin in bundles at sites distant from adhesion sites.

A similar co-linear relationship for the 140K, fibronectin, and membrane-associated cytoskeletal proteins at ECM contacts was observed after CEF and CEL cells were cultured in the presence of 0.3% serum, a condition reported to enrich elongated ECM contacts (40). These co-distribution data for the 140K in our double-label and triple-label immunofluorescent studies are consistent with and complementary to a previous single-label immunoelectron microscopic study that used the ultrathin frozen-sectioning method that did not involve detergent for permeabilization of cells and that showed specific localization of 140K to the plasma membrane, particularly at the close contacts and ECM contacts of fibroblast-substratum interfaces (12). Together, these results

FIGURE 5 Correlative IRM and triple-label immunofluorescence for 140K, tropomyosin (TM), and fibronectin (FN) in CEL cells cultured for 1 d. Arrows point to the focal adhesion sites in IRM that are termini of the MFBs; 140K, TM, and FN labelings surround these focal adhesion sites. Arrowheads point to linear regions of microfilaments away from their membrane attachment sites as determined by IRM that are labeled for TM and sometimes for FN, but not for 140K. × 1,200.
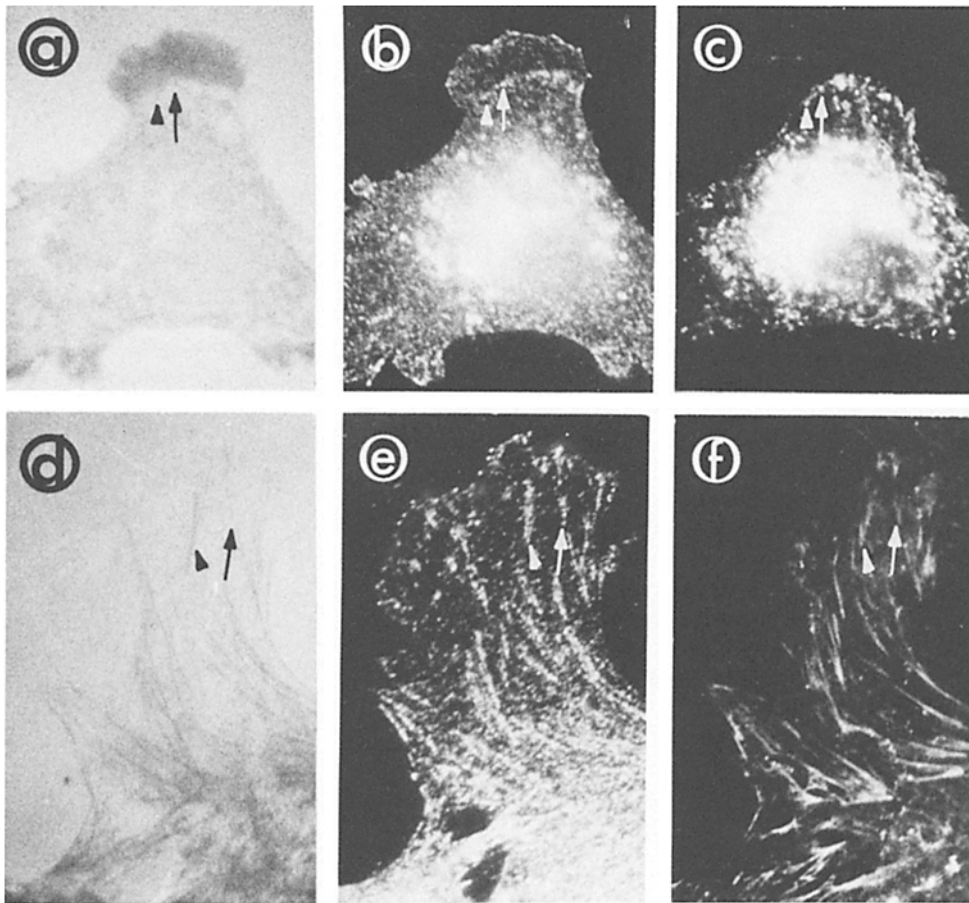
strongly suggest the involvement of 140K aggregates in a cell surface linkage complex between intracellular α-actinin-containing microfilaments and extracellular fibronectin fibrils.

Formation of Cell Surface Linkage Complexes in Spreading Cells

As described above, an α-actinin–140K–fibronectin association at the ECM contacts can be readily observed in stationary CEF and CEL cells. We have used this model system to examine the initial establishment of such ECM contact sites in spreading cells examined 1–6 h after they were seeded. CEF cultured on glass coverslips were recorded on 35-mm film at one frame per minute at 37°C with IRM to study their history and inventory of contacts with the substratum. The same cells were fixed, relocated by a previously described procedure (7), and then examined with double-label immunofluorescence by pairwise labeling with α-actinin and 140K, 140K and fibronectin, or α-actinin and fibronectin. Examples of the time course of appearance of ECM contacts are shown in Fig. 6, a–f for 140K-fibronectin spatial associations and in Fig. 7, a–f for α-actinin–fibronectin associations. In more than 60 cases examined, we detected such associations in 41 cells as judged by IRM and co-localizations of intracellular and extracellular antigens, which appeared under the cells posterior to the marginal close contacts within 30 min after cells were seeded (Fig. 6, a–c; Fig. 7, a–c). As cells undergo spreading, the ECM contacts are known to elongate centripetally in spatial association with cytoskeletal fibers (27, 28). Within 6 h, the 140K antigen was found to aggregate or concentrate at elongated ECM contacts, and α-actinin and

fibronectin clearly became spatially associated with them (Fig. 6, d–f; Fig. 7, d–f). The association, frequently centrad, of 140K with ECM contacts (Figs. 4–7), may be associated with the centripetal extension of microfilament bundles (27, 28).

Involvement of 140K in Cellular Adhesion to Fibronectin Substrata

The effects of JG22E on fibronectin-mediated cellular adhesion and spreading of CEF were tested as outined in Materials and Methods. CEF attached and spread on fibronectin-coated substrata in a concentration-dependent manner (Fig. 8 a; see also references 5, 18, 35, and 36). When JG22E monoclonal antibodies were added to CEF suspensions during this cell adhesion assay, we found that fibronectin-mediated cellular adhesion and spreading was inhibited by >80% relative to background by JG22E (Fig. 8 a). Increasing the concentration of JG22E did not increase inhibition (Fig. 8 a). These findings suggested a functional association of fibronectin with 140K during cell attachment and spreading.

We then compared the effects of JG22E on fibronectin-mediated cell adhesion and spreading of normal and RSV-transformed CEF (Fig. 8 b). JG22E monoclonal antibody also markedly inhibited fibronectin-mediated adhesion and spreading of transformed CEF. However, a slightly decreased effectiveness of the antibody at higher concentrations was detected with these transformed cells (Fig. 8 b). One possible explanation for the decrease in inhibition of adhesion to fibronectin with increased amounts of antibody is that the antibody becomes adsorbed to the substratum and itself begins to function as a positive mediator of adhesion (19). If the
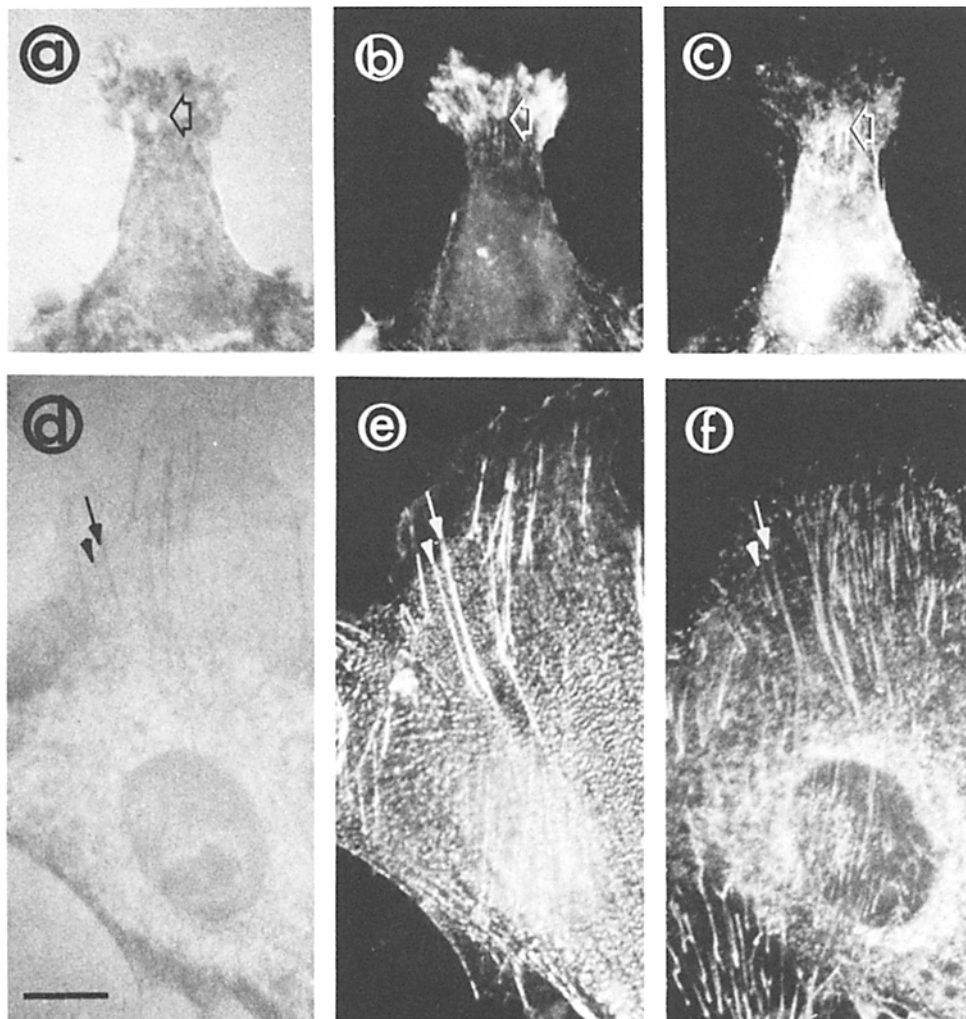
FIGURE 7 Formation of α-actinin–fibronectin complexes as shown by intracellular α-actinin and extracellular fibronectin co-distribution in early spreading CEF. (a–c) IRM (a) and double-immunofluorescent labeling for α-actinin (b) and fibronectin (c) of a cell cultured for 1 h. All images were focused at the same level, i.e., at the cell-substratum interface. Open arrows indicate the appearance of the α-actinin–fibronectin complexes under the cell posterior to the marginal close contacts (a) as shown by coincident labeling of α-actinin (b) and fibronectin (c) at these sites. (d–f) IRM (d) and double labeling for α-actinin (e) and fibronectin (f) of a cell cultured for 6 h. Arrow and arrowhead pairs indicate elongated ECM contacts (d) that were labeled for both α-actinin (e) and fibronectin (f). × 1,200.

JG22E monoclonal antibody alone was adsorbed to substrata in the absence of fibronectin, the adsorbed antibody itself could mediate some cell attachment and spreading for both normal and transformed CEF (Fig. 8, c and d). If the antibody was cross-linked to the substratum by glutaraldehyde to prevent its release into solution during the assay, it became even more effective as a mediator of cell adhesion (Fig. 8, c and d). A similar enhancement of activity after the monoclonal antibody was cross-linked to a substratum was found in comparisons of such glutaraldehyde cross-linking with gelatin, and of carbodiimide cross-linking with 1-ethyl-3(3-dimethylaminopropyl)carbodiimide to a tissue culture plastic substratum.

DISCUSSION

We have analyzed the localization and function of the 140K proteins that are identified by the JG22E monoclonal antibody. Several lines of evidence strongly suggest that the 140K proteins are somehow involved in cell surface linkage complexes that associate MFBs inside cells with fibronectin fibrils outside cells. The evidence can be summarized as follows. (a) Monoclonal antibodies initially raised against chicken myoblasts, i.e., JG9, JG22 (17), JG22E, and CSAT from another laboratory (32), when added to culture medium, cause myoblasts to round-up. Since myoblasts are reported to require fibronectin for attachment and spreading on substrata (13), these monoclonal antibodies may block fibronectin-mediated

cellular adhesion and spreading. (b) In this paper, a direct test of this hypothesis with fibroblasts showed that the JG22E monoclonal antibody inhibited fibronectin-mediated adhesion and spreading of normal and transformed fibroblasts. Similar results are apparently obtained with the related CSAT monoclonal antibody (reference 14a and unpublished work cited therein). (c) Analogous to the dualistic nature of fibronectin itself (48), moreover, this inhibitory JG22E antibody can also become a mediator of cell adhesion if appropriately attached to a substrate; this finding rules out the possibility that JG22E merely inhibits all cell-spreading responses. (d) These monoclonal antibodies affinity purify a complex of three to four proteins averaging 140K in apparent size only from detergent extracts of cells or embryos but not from various salt or urea extracts (6, 8, 17, 29, 30, 32). The three components can be metabolically labeled with [³H]glucosamine or externally with ¹²⁵I, which suggests that they are glycoprotein in nature (6, 30). Direct immunoelectron microscopic labeling of the 140K antigen by use of JG22 monoclonal antibody shows localization to the plasma membrane at cell-to-ECM contact sites (12). The above findings are consistent with the integral membrane nature of the 140K. (e) By double-label and triple-label immunofluorescence combined with IRM to locate cell-to-ECM contact sites (ECM contacts), we observed in the present study a co-localization of the 140K with fibronectin fibrils and MFBs at the ECM contacts in cultured fibroblasts, and this correlation was traced through-
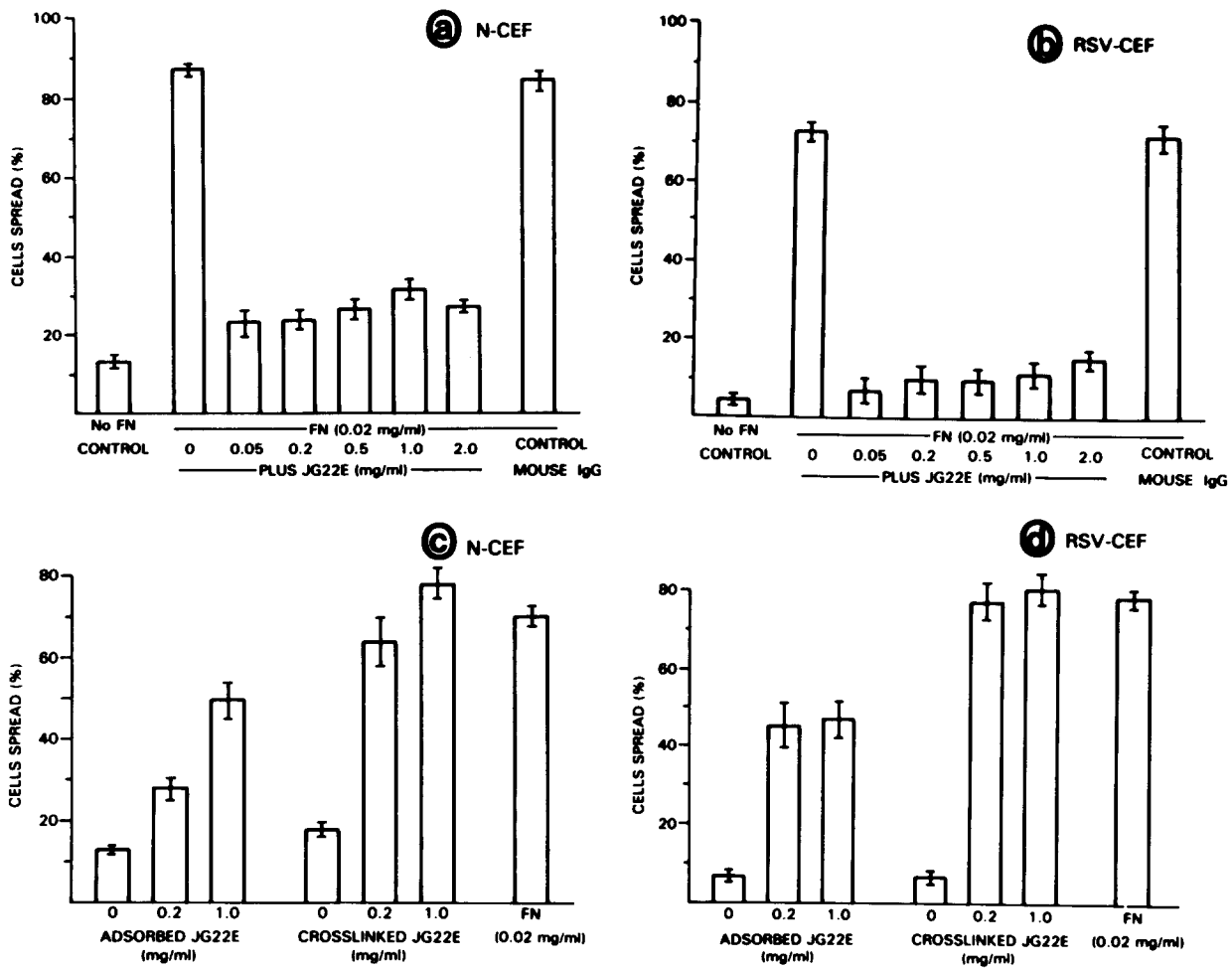
FIGURE 8   Inhibition of fibronectin (FN)-mediated cellular adhesion and spreading by the monoclonal antibody JG22E directed against 140K in normal CEF (N-CEF) (a) and RSV-CEF (b) and the effects of JG22E on cellular adhesion and spreading in normal CEF (c) and RSV-CEF (d). (a and b) Attachment and spreading of CEF (a) and RSV-CEF (b) on fibronectin-coated plastic surfaces in the presence of JG22E at various concentrations. (c and d) Attachment and spreading of CEF (c) and RSV-CEF (d) on either JG22E-coated or JG22E-cross-linked surfaces. Each data point represents the mean of three determinations.

out early spreading events. In a separate experiment, we observed that there was a decrease in the number of ECM contacts and an induction of rosette contacts in CEF transformed by RSV as reported in other RSV-transformed cells (14). Loss of cell surface fibronectin (24, 34, 46) from rosette contacts of RSV-transformed CEF (11) occurred concomitantly with a redistribution of 140K and α-actinin (unpublished results). A comparable localization study that used the CSAT monoclonal antibody was not possible, because CSAT lacks reactivity with fixed cells (32). (f) Polyclonal antibodies directed against JG22E affinity-purified 140K proteins show similar localization patterns and inhibitory effects on cellular adhesion to fibronectin substrata. Together, these data suggest that the 140K aggregates or one component of the complex may interact with fibronectin outside of the cell and with cytoskeletal elements inside.

From our immunolocalization data of 140K membrane proteins and the other evidence presented above, the 140K proteins are a possible candidate for the important role of integral proteins involved in the transmembrane linkage connecting MFBs and fibronectin fibrils to the membrane, although other functions are possible. In rounded cells or on the dorsal surface of spread cells, the 140K is diffusely scattered at the cell surface (12). Concomitant with the spreading

induced either by fibronectin or by JG22E immobilized on the substratum, cells may acquire linear accumulations of the 140K and highly ordered intracellular MFBs and extracellular fibronectin fibrils at ECM contacts (Figs. 4 and 5). When fibronectin is lost from the membrane, as in transformed cells (25, 34, 46), cells undergoing cytokinesis, and trypsinized cells, the cells may reduce the number of ECM contacts and focal adhesions and return to the rounded state with diffuse 140K and submembranous microfilaments. Further tests will be required to establish definitively whether the 140K proteins are indeed these crucial transmembrane linkage molecules, although our data appear to establish them as a leading candidate.

REFERENCES

1. Ali, I. U., V. M. Mautner, R. P. Lanza, and R. O. Hynes. 1977. Restoration of normal morphology, adhesion, and cytoskeleton in transformed cells by addition of a transformation-sensitive surface protein. Cell. 11:115-126.
2. Avnur, Z., and B. Geiger. 1981. The removal of extracellular fibronectin from areas of cell-substrate contact. Cell. 25:121-132.
3. Burnette, W. N. 1981. "Western Blotting": electrophoretic transfer of proteins from sodium dodecyl sulfate-polyacrylamide gels to unmodified nitrocellulose and radiographic detection with antibody and radiolabeled protein A. Anal. Biochem. 112:195-203.
4. Burridge, K., and J. R. Feramisco. 1980. Micro-injection and localization of a 130K protein in living fibroblasts. Cell. 19:587-596.
5. Carter, W. G., H. Rauvala, and S.-I. Hakomori. 1981. Studies on cell adhesion and recognition. II. The kinetics of cell adhesion and cell spreading on surface coated with carbohydrate-reactive proteins (glycosidases and lectins) and fibronectin. J. Cell Biol. 88:138-148.
6. Chapman, A. E. 1984. Characterization of a 140 Kd cell surface glycoprotein involved in myoblast adhesion. J. Cell. Biochem. 25:109-121.
7. Chen, W.-T. 1981. Mechanism of retraction of the trailing edge during fibroblast movement. J. Cell Biol. 90:187-200.
8. Chen, W.-T., A. Chapman, S. J. Singer, J. Greve, and D. I. Gottlieb. 1981. A monoclonal antibody directed to a 140 Kd surface glycoprotein immunolabels sites of close contacts between cultured fibroblasts and their substrata. J. Cell Biol. 91(2, pt. 2):258a (Abstr.).
9. Chen, W.-T., and S. J. Singer. 1980. Fibronectin is not present in the focal adhesions formed between normal cultured fibroblasts and their substrata. Proc. Natl. Acad. Sci. USA. 77:7318-7322.
10. Chen, W.-T., and S. J. Singer. 1982. Immunoelectron microscopic studies of the sites of cell-substratum and cell-cell contacts in cultured fibroblasts. J. Cell Biol. 95:205-222.
11. Chen, W.-T., K. Olden, B. A. Bernard, and F.-F. Chu. 1984. Expression of transformation-associated protease(s) that degrade fibronectin at cell contact sites. J. Cell Biol. 98:1546-1555.
12. Chen, W.-T., J. M. Greve, D. I. Gottlieb, and S. J. Singer. 1985. The immunocytochemical localization of 140 Kd cell adhesion molecules in cultured chicken fibroblasts, and in chicken smooth muscle and intestinal epithelial tissues. J. Histochem. Cytochem. In press.
13. Chiquet, M., E. C. Puri, and D. C. Turner. 1979. Fibronectin mediates attachment of chicken myoblasts to a gelatin-coated substratum. J. Biol. Chem. 254:5475-5482.
14. David-Pfeuty, T., and S. J. Singer. 1980. Altered distributions of the cytoskeletal proteins vinculin and α-actinin in cultured fibroblasts transformed by Rous sarcoma virus. Proc. Natl. Acad. Sci. USA. 77:6687-6691.
14a. Decker, C., R. Greggs, K. Duggan, J. Stubbs, and A. Horwitz. 1984. Adhesive multiplicity in the interaction of embryonic fibroblasts and myoblasts with extracellular matrices. J. Cell Biol. 99:1398-1404.
15. Furcht, L. T. 1983. Structure and function of the adhesive glycoprotein fibronectin. In Modern Cell Biology. B. Satir, editor. Alan B. Liss, Inc., New York. 53-117.
16. Geiger, B., A. H. Dutton, K. T. Tokuyasu, and S. J. Singer. 1981. Immunoelectron microscope studies of membrane-microfilament interactions: distributions of α-actinin, tropomyosin, and vinculin in intestinal epithelial brush border and chicken gizzard smooth muscle cells. J. Cell Biol. 91:614-628.
17. Greve, J. M., and D. I. Gottlieb. 1982. Monoclonal antibodies which alter the morphology of cultured chick myogenic cells. J. Cell. Biochem. 18:221-229.
18. Grinnell, F., and D. G. Hays. 1978. Cell adhesion and spreading factor. Similarity to cold insoluble globulin in human serum. Exp. Cell Res. 115:221-229.
19. Grinnell, F., and D. G. Hays. 1978. Induction of cell spreading by substratum-adsorbed ligands directed against the cell surface. Exp. Cell Res. 116:275-284.
20. Heggeness, M. H., J. F. Ash, and S. J. Singer. 1978. Transmembrane linkage of fibronectin to intracellular actin-containing filaments in cultured human fibroblasts. Ann. NY Acad. Sci. 312:414-447.
21. Horwitz, A., N. Neff, A. Sessions, and C. Decker. 1982. Cellular interactions in myogenesis. In Muscle Development. Cold Spring Harbor Laboratory, Cold Spring Harbor, NY. 291-300.
22. Hynes, R. O. 1981. Relationships between fibronectin and the cytoskeleton. Cell Surf. Rev. 7:97-136.
23. Hynes, R. O., and A. T. Destree. 1978. Relationships between fibronectin (LETS protein) and actin. Cell. 15:875-886.
24. Hynes, R. O., A. T. Destree, and D. D. Wagner. 1982. Relationships between microfilaments, cell-substratum adhesion, and fibronectin. Cold Spring Harbor Symp. Quant. Biol. 46:659-670.
25. Hynes, R. O., and A. Wyke. 1975. Alterations in surface proteins in chicken cells transformed by temperature-sensitive mutants of Rous sarcoma virus. Virology. 64:492-504.
26. Hynes, R. O., and K. M. Yamada. 1982. Fibronectins: multifunctional modular glycoproteins. J. Cell Biol. 95:369-377.
27. Izzard, C. S., and L. R. Lochner. 1976. Cell-to-substrate contacts in living fibroblasts: an interference reflexion study with an evaluation of the technique. J. Cell Sci. 21:129-159.
28. Izzard, C. S., and L. R. Lochner. 1980. Formation of cell-to-substrate contacts during fibroblast motility: an interference reflexion study. J. Cell Sci. 42:81-116.
29. Knudsen, K. A., C. A. Buck, C. H. Damsky, and A. F. Horwitz. 1982. Adhesion-related glycoproteins isolated using a monoclonal antibody. J. Cell Biol. 95(2, pt.2):111a (Abstr.).
30. Knudsen, K. A., A. F. Horowitz, and C. A. Buck. 1985. A monoclonal antibody identifies a glycoprotein complex involved in cell-substratum adhesion. Exp. Cell Res. In press.
31. Mosher, D. F., editor. 1985. Fibronectin. Academic Press, Inc., New York. In press.
32. Neff, N. T., C. Lowrey, C. Decker, A. Tovar, C. Damsky, C. Buck, and A. F. Horwitz. 1982. A monoclonal antibody detaches embryonic skeletal muscle from extracellular matrices. J. Cell Biol. 95:654-666.
33. Oesch, B., and W. Birchmeier. 1982. New surface component of fibroblast's focal contacts identified by a monoclonal antibody. Cell. 31:671-679.
34. Olden, K., and K. Yamada. 1977. Mechanism of the decrease in the major cell surface protein of chick embryo fibroblasts after transformation. Cell. 11:957-969.
35. Pena, S. D. J., and R. C. Hughes. 1978. Fibronectin-plasma membrane interactions in the adhesion and spreading of hamster fibroblasts. Nature (Lond.) 276:80-82.
36. Rauvala, H., W. G. Carter, and S.-I. Hakomori. 1981. Studies on cell adhesion and recognition. I. Extent and specificity of cell adhesion triggered by carbohydrate-reactive proteins (glycosidases and lectins) and by fibronectin. J. Cell Biol. 88:127-137.
37. Ruoslahti, E., E. Engvall, and E. G. Hayman. 1981. Fibronectin: current concepts of its structure and functions. Collagen Relat. Res. 1:95-128.
38. Ruoslahti, E., E. G. Hayman, P. Kuusela, J. E. Shively, and E. Engvall. 1979. Isolation of a tryptic fragment containing the collagen-binding site of plasma fibronectin. J. Biol. Chem. 254:6054-6059.
39. Singer, I. I. 1979. The fibronexus: a transmembrane association of fibronectin-containing fibers and bundles of 5 nm microfilaments in hamster and human fibroblasts. Cell. 16:675-685.
40. Singer, I. I. 1982. Association of fibronectin and vinculin with focal contacts and stress fibers in stationary hamster fibroblasts. J. Cell Biol. 92:398-408.
41. Singer, I. I., and P. R. Paradiso. 1981. A transmembrane relationship between fibronectin and vinculin (130 kd protein): serum modulation in normal and transformed hamster fibroblasts. Cell. 24:481-492.
42. Singer, S. J., and W.-T. Chen. 1983. Molecular interactions at cell-substratum and cell-cell contacts formed by cultured fibroblasts. In Falk Symposium on Structural Carbohydrates of Liver. MTP Press Ltd., Hingham, MA. 199-208.
43. Sugrue, S. P., and E. D. Hay. 1982. Interaction of embryonic corneal epithelium with exogenous collagen, laminin, and fibronectin: role of endogenous protein synthesis. Dev. Biol. 92:97-106.
44. Vollmers, H. P., and W. Birchmeier. 1983. Monoclonal antibodies inhibit the adhesion of mouse B16 melanoma cells in vitro and block lung metastases in vivo. Proc. Natl. Acad. Sci. USA. 80:3729-3733.
45. Willingham, M. C., K. M. Yamada, S. S. Yamada, J. Pouyssegur, and I. Pastan. 1977. Microfilament bundles and cell shape are related to adhesiveness to substratum and are dissociable from growth control in cultured fibroblasts. Cell. 10:375-380.
46. Yamada, K. M. 1978. Immunological characterization of a major transformation-sensitive fibroblast cell surface glycoprotein: localization, redistribution, and role in cell shape. J. Cell Biol. 78:520-541.
47. Yamada, K. M. 1983. Cell surface interactions with extracellular materials. Annu. Rev. Biochem. 52:761-800.
48. Yamada, K. M., and D. W. Kennedy. 1984. Dualistic nature of adhesive protein function: fibronectin and its biologically active peptide fragments can autoinhibit fibronectin function. J. Cell Biol. 99(1, Pt.1):29-36.